Shock-tuned cryogenic-deuterium-tritium implosion performance on Omega[a)]

T. C. Sangster,[1,b)] V. N. Goncharov,[1,c)] R. Betti,[1,c),d)] T. R. Boehly,[1] D. T. Casey,[2] T. J. B. Collins,[1] R. S. Craxton,[1] J. A. Delettrez,[1] D. H. Edgell,[1] R. Epstein,[1] K. A. Fletcher,[3] J. A. Frenje,[2] Y. Yu. Glebov,[1] D. R. Harding,[1,e)] S. X. Hu,[1] I. V. Igumenschev,[1] J. P. Knauer,[1] S. J. Loucks,[1] C. K. Li,[2] J. A. Marozas,[1] F. J. Marshall,[1] R. L. McCrory,[1,c)] P. W. McKenty,[1] D. D. Meyerhofer,[1,c)] P. M. Nilson,[1] S. P. Padalino,[3] R. D. Petrasso,[2] P. B. Radha,[1] S. P. Regan,[1] F. H. Seguin,[2] W. Seka,[1] R. W. Short,[1] D. Shvarts,[1,4] S. Skupsky,[1] V. A. Smalyuk,[1,f)] J. M. Soures,[1] C. Stoeckl,[1] W. Theobald,[1] and B. Yaakobi[1]

[1]*Laboratory for Laser Energetics, University of Rochester, 250 East River Road, Rochester, New York 14623, USA*

[2]*Massachusetts Institute of Technology, Plasma Science and Fusion Center, Cambridge, Massachusetts 02139, USA*

[3]*Department of Physics and Astronomy, State University of New York, Geneseo, New York 14454, USA*

[4]*Nuclear Research Center Negev, IL-84190 Beer Sheva, Israel*

(Received 16 December 2009; accepted 22 February 2010; published online 23 April 2010)

Cryogenic-deuterium-tritium (DT) target compression experiments with low-adiabat (α), multiple-shock drive pulses have been performed on the Omega Laser Facility [T. R. Boehly, D. L. Brown, R. S. Craxton *et al.*, Opt. Commun. **133**, 495 (1997)] to demonstrate hydrodynamic-equivalent ignition performance. The multiple-shock drive pulse facilitates experimental shock tuning using an established cone-in-shell target platform [T. R. Boehly, R. Betti, T. R. Boehly *et al.*, Phys. Plasmas **16**, 056301 (2009)]. These shock-tuned drive pulses have been used to implode cryogenic-DT targets with peak implosion velocities of 3×10^7 cm/s at peak drive intensities of 8×10^{14} W/cm^2. During a recent series of $\alpha\sim2$ implosions, one of the two necessary conditions for initiating a thermonuclear burn wave in a DT plasma was achieved: an areal density of approximately 300 mg/cm^2 was inferred using the magnetic recoil spectrometer [J. A. Frenje, C. K. Li, F. H. Séguin *et al.*, Phys. Plasmas **16**, 042704 (2009)]. The other condition—a burn-averaged ion temperature $\langle T_i\rangle_n$ of 8–10 keV—cannot be achieved on Omega because of the limited laser energy; the kinetic energy of the imploding shell is insufficient to heat the plasma to these temperatures. A $\langle T_i\rangle_n$ of approximately 3.4 keV would be required to demonstrate ignition hydrodynamic equivalence [Betti *et al.*, Phys. Plasmas **17**, 058102 (2010)]. The $\langle T_i\rangle_n$ reached during the recent series of $\alpha\sim2$ implosions was approximately 2 keV, limited primarily by laser-drive and target nonuniformities. Work is underway to improve drive and target symmetry for future experiments. © *2010 American Institute of Physics*. [doi:10.1063/1.3360928]

I. INTRODUCTION

Experiments are underway on the National Ignition Facility (NIF) (Ref. 1) to tune hohlraum symmetry in preparation for the first attempts at inertial confinement fusion (ICF) ignition with cryogenic-deuterium-tritium (DT) capsules[2] in late 2010. For the past several years, direct-drive, energy-scaled, and cryogenic-DT and D_2 implosions have been performed on the Omega Laser Facility[3] to demonstrate hydrodynamic-equivalent ignition performance.[4–14] Hydrodynamic equivalence on Omega implies that design parameters such as implosion velocity, in-flight aspect ratio, and laser-drive intensity are the same as those for a high-gain ignition design on the NIF.[15] In other words, the core stagnation conditions (peak pressure and density) for hydrodynamically equivalent implosions on the two facilities would be the same; only the laser energy would be different. For a given set of design parameters, the core stagnation conditions result in a burn-averaged fuel areal density $\langle\rho R\rangle_n$ and burn-averaged ion temperature $\langle T_i\rangle_n$ that can be measured experimentally to confirm hydrodynamically equivalent ignition performance on Omega. Here, the burn-averaged notation $\langle\ \rangle_n$ indicates that the areal density and ion temperature are time-integrated averages over the neutron emission time or fusion burn; for the ion temperature, this also implies a spatial or volume average over the burning plasma. Zhou and Betti[16] derived an ICF-equivalent of the Lawson criterion[17] for burning plasmas based on these experimental observables:

$$\langle\rho R\rangle_n^{\text{no-}\alpha}[\langle T_i^{\text{no-}\alpha}\rangle_n/4.6]^2>1, \tag{1}$$

[a)]Paper NI2 2, Bull. Am. Phys. Soc. **54**, 179 (2009).
[b)]Invited speaker.
[c)]Also at: Department of Physics and Astronomy, University of Rochester.
[d)]Also at: Department of Mechanical Engineering, University of Rochester.
[e)]Also at: Department of Chemical Engineering, University of Rochester.
[f)]Present address: Lawrence Livermore National Laboratory, Livermore, CA.

where the "no-α" superscript implies no additional fuel heating from α-particle deposition in the compressed fuel and the units are g/cm^2 for the areal density and keV for the ion temperature. The ignition hydrodynamic equivalence values for $\langle \rho R \rangle_n$ and $\langle T_i \rangle_n$ using the laser energy available at Omega are derived analytically in Ref. 15. The Omega requirements for ignition hydroequivalence are a $\langle \rho R \rangle_n$ of approximately 300 mg/cm^2 and an $\langle T_i \rangle_n$ of 3.4 keV.

The cryogenic-DT experiments reported here were designed to achieve high-areal densities and ion temperatures. This paper reports a measurement of $\langle \rho R \rangle_n$ of approximately 300 ± 60 mg/cm^2 on a low-adiabat ($\alpha \sim 2$) cryogenic-DT implosion with an implosion velocity of $\sim 3 \times 10^7$ cm/s. This areal density is one of the requirements for demonstrating ignition hydroequivalence on Omega (in the next section, it will be shown that this target design scales to ignition on the NIF). This is also the minimum areal density required to initiate a thermonuclear burn wave in a DT plasma.[18] The specific target design and the shock tuning required to achieve the design adiabat and implosion velocity are discussed in Sec. II; measurement of $\langle \rho R \rangle_n$ and $\langle T_i \rangle_n$ is discussed in Sec. III. Results are summarized in Sec. IV.

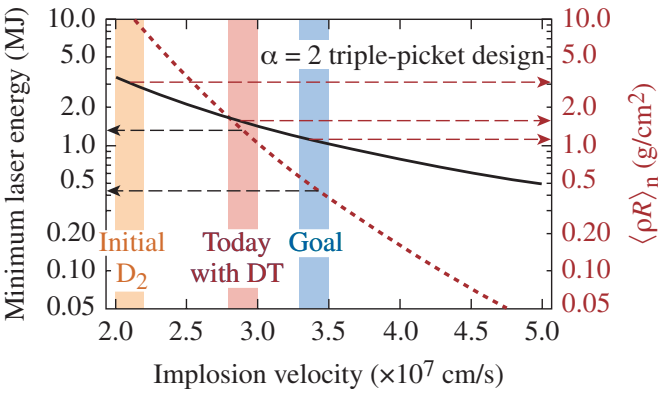

FIG. 1. (Color) The minimum laser energy for ignition (black curve) and the corresponding minimum areal density (red curve) are plotted as functions of the implosion velocity for a $\alpha \sim 2$ design. Although the energy-scaled experiments on Omega (Ref. 7) with implosion velocities of $\sim 2 \times 10^7$ cm/s do not scale to ignition with existing facilities, the minimum laser energy for ignition with the current energy-scaled experiments at $\sim 3 \times 10^7$ is 1.5 MJ, well within the design envelope of the NIF. Future energy-scaled experiments at $\sim 3.5 \times 10^7$ cm/s are expected to scale to ignition with a reasonable margin (much lower minimum ignition energy than the facility can produce).

II. TARGET DESIGN FOR IGNITION HYDRODYNAMIC EQUIVALENCE ON OMEGA

The $\langle \rho R \rangle_n$ in an ICF implosion depends primarily on laser energy (E_L) and the adiabat of the fuel shell during acceleration,[19,20]

$$\langle \rho R \rangle_n \sim 1.67 (E_L)^{0.33} \alpha^{-0.54}, \tag{2}$$

where E_L is in megajoule. To form a hot spot and initiate a burn wave through the main fuel, the laser energy must exceed a minimum threshold value that can be written as[19,20]

$$(E_L)_{\min} \sim 0.7 (I_{\text{peak}})^{0.25} \alpha^{1.9} (V_{\text{imp}}/3 \times 10^7)^{-6.6} \times (P_{\text{drive}}/100)^{-0.77} \tag{3}$$

for a plastic ablator, where E_L is in megajoule, the peak drive intensity I_{peak} is in units of 10^{15} W/cm^2, the implosion velocity V_{imp} is in units of cm/s, and the peak drive pressure P_{drive} is in units of Mbar. The minimum areal density required for ignition can be derived by inserting Eq. (3) into Eq. (2),

$$(\langle \rho R \rangle_n)_{\min} \sim 1.5 (V_{\text{imp}}/3 \times 10^7)^{-2.14} \times (I_{\text{peak}})^{0.08} \alpha^{0.09} (P_{\text{drive}}/100)^{-0.26}. \tag{4}$$

Equation (4) shows that for drive pressures of the order of 100 Mbar, the minimum required areal density depends primarily on the implosion velocity. The minimum laser energy and fuel areal density required for ignition are plotted in Fig. 1 as a function implosion velocity for fixed values of the fuel adiabat, the peak drive intensity, and the peak drive pressure. Three regions corresponding to V_{imp} from past, current, and future experiments are identified.

In 2007, a series of low-adiabat implosions using cryogenic-D$_2$ fuel produced a $\langle \rho R \rangle_n \sim 200$ mg/cm^2 (Ref. 7). These targets were imploded using an 18-kJ continuous pulse with $I_{\text{peak}} \sim 5 \times 10^{14}$ W/cm^2 and $\alpha \sim 2.5$ (Ref. 6). The fuel mass led to a $V_{\text{imp}} \sim 2.2 \times 10^7$ cm/s (these experiments correspond to the orange shaded region in Fig. 1; the width of the shaded region represents uncertainty in the absorbed energy and measured bang time). These implosions do not scale to ignition on the NIF (e.g., a minimum laser energy >10 MJ is required), although at the time, they produced the highest fuel densities ever measured in laboratory-based ICF implosions.

Recent low-adiabat ($\alpha \sim 2$) implosions using cryogenic-DT fuel have produced a $\langle \rho R \rangle_n \sim 300$ mg/cm^2 (details are discussed in Sec. III). These implosions were driven using a 25-kJ multiple-picket pulse (described below) with $I_{\text{peak}} \sim 8 \times 10^{14}$ W/cm^2, resulting in a $V_{\text{imp}} \sim 3 \times 10^7$ cm/s (the red shaded region in Fig. 1). These are the first target designs for Omega that scale directly to ignition on the NIF (i.e., the minimum laser energy for ignition is within the NIF design envelope). A 15% increase in the implosion velocity (the blue shaded region in Fig. 1) will be necessary to make this design robust (i.e., the minimum laser energy for ignition would be about 0.5 MJ). These experiments are planned for the near future.

The target and the drive-pulse design for recent high-areal-density implosions on Omega are energy scaled from a new direct-drive-ignition design developed by Goncharov *et al.*[21] The target, shown in Fig. 2(a), is based on a thick plastic ablator to minimize hot-electron preheat (the laser pulse does not burn through the plastic until the end of the drive pulse,[5] maximizing the ratio of the coronal electron temperature to the electron-density scale length). The new drive pulse, shown in Fig. 2(b), is a multiple-shock (4×), multiple-picket design similar in concept to that developed for indirect-drive ignition on the NIF.[2] For a laser energy of 1.5 MJ, this target is predicted to ignite and produce a gain of 48. The multiple-picket design is motivated primarily by the desire to minimize shock preheating of the fuel.

The pickets launch a series of decaying shocks that are

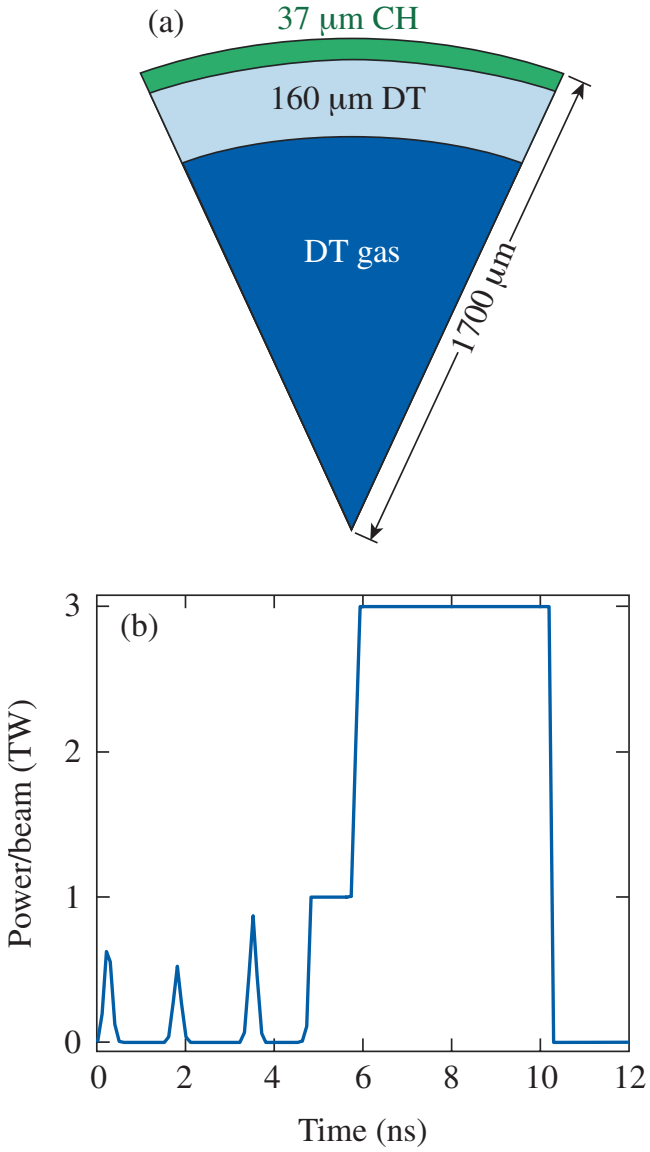

FIG. 2. (Color) A new direct-drive-ignition target design has been developed by Goncharov *et al.* (Ref. 22). (a) Details of the target and (b) the multiple-picket, multiple-shock drive pulse for this target. The design adiabat is approximately 2.

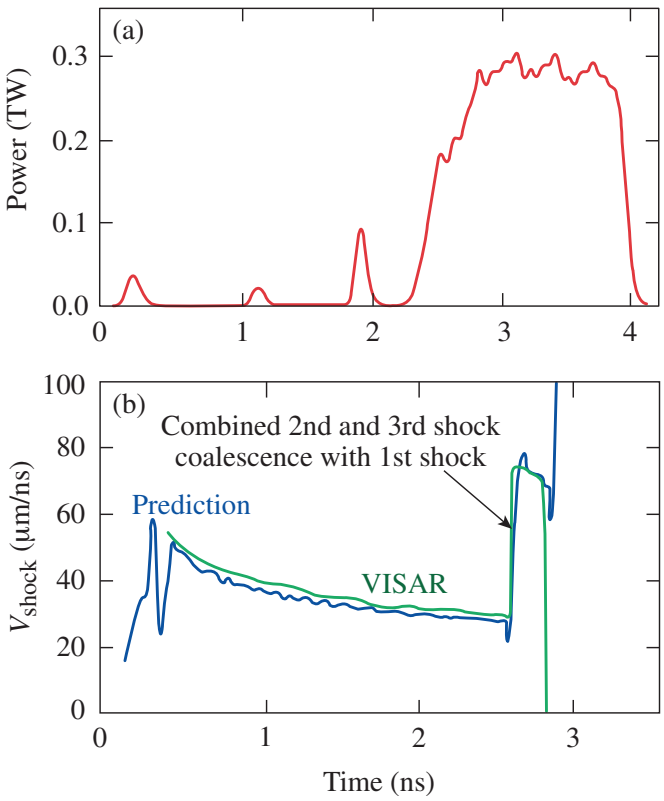

FIG. 3. (Color) (a) The Omega energy-scaled version of the ignition-drive pulse from Fig. 2(b). This pulse was used to perform a shock-timing measurement using a spherical cone-in-shell target (Ref. 23). The third picket (at about 2 ns) is approximately 20% higher than designed. The third shock catches up with the first and second shocks too early, resulting in the coalesced shock in (b) at 2.7 ns (the green trace). The measured shock velocity is in excellent agreement with the 1D radiation-hydrocode prediction (blue trace).

designed to coalesce simultaneously with the main drive at the inner surface of the cold fuel. A velocity interferometer system for any reflector (VISAR)-based shock-tuning platform developed by Boehly *et al.*[22] for hohlraum-based ignition targets has been adapted to measure the shock propagation and coalescence in a direct-drive spherical geometry. A cone-in-plastic-shell target is completely filled with liquid deuterium (the plastic shell is identical to those used for cryogenic targets on Omega) and irradiated using most of the Omega beams (except for those that would intercept the cone). A window at the wide end of the cone provides an optical path for the VISAR probe laser to reflect off the converging shock propagating through the shell. If the shocks are tuned properly (by adjusting the picket energies and temporal spacing), the VISAR records a single strong velocity shift at a time commensurate with propagation through the ice layer. If the shocks are not tuned properly, the VISAR will record a series of weaker velocity shifts as the various shocks catch up to the leading shock. An example of an improperly tuned multiple-picket drive pulse is shown in Fig. 3(a). In Fig. 3(b), the shock velocity measured using the VISAR is plotted as a function of time for a liquid-deuterium-filled cone-in-shell target and the drive pulse shown in Fig. 3(a). In this example, the third picket shock is too strong and overtakes the second and first shocks too quickly. The velocity of the resulting shock (~75 μm/ns) is used to distinguish between a stronger/weaker second or third shock (for a properly tuned pulse, all of the shocks would coalesce simultaneously at around 3 ns with a resulting shock velocity of approximately 120 μm/ns). By adjusting the individual picket energies, it is possible to control the fuel adiabat throughout the pulse. This is an essential step in achieving high fuel compression and perhaps the primary advantage of the new multiple-shock design.

III. HIGH $\langle \rho R \rangle_n$ IMPLOSIONS ON OMEGA

Measuring the areal density of highly compressed cryogenic-DT fuel is a relatively new challenge for the ICF program, and there are few options available. It should be possible to generate a transmission Compton radiograph[23] of

the cold-fuel distribution at peak compression using high-energy x rays (75–100 keV) generated by a short-pulse IR laser. Such radiographs would provide a two-dimensional (2D) projection of the fuel-density distribution at peak compression. A kilojoule-class short-pulse laser (of the order of 10 ps) would be used to generate the intense burst of x rays needed to provide adequate contrast and to avoid motional blurring. The development of this technique for implosions on Omega is ongoing but has yet to be demonstrated with cryogenic fuels.

The burn-averaged areal density can be inferred using the primary fusion neutrons as an "internal" backlighter source. For example, the number of primary 14-MeV neutrons scattered in the dense fuel is proportional to the fuel areal density during the burn.[24] A magnetic recoil spectrometer (MRS) was recently installed on Omega to measure the primary and scattered neutron yields in cryogenic-DT implosions.[25] Neutrons emitted from the target forward scatter deuterons from a CD foil mounted close to the target. These forward-scattered deuterons are momentum analyzed using a magnet and an array of detectors to generate a deuteron spectrum that is directly proportional to the emitted neutron spectrum (classical two-body scattering kinematics). The energy range of the scattered neutron yield measurement is typically 10 to 13 MeV (corresponding to a deuteron energy range of approximately 6–9 MeV) as the neutrons from T+T fusion contaminate the spectrum below 9.5 MeV (this limits the solid angle of the probed areal density). The response function of the spectrometer is determined from accurate measurements of the bending magnet field and the geometric location of the scattering foil relative to the magnet aperture and the detector plane. The primary systematic uncertainty in the scattered yield is the (n, D) elastic-scattering cross section. In practice, counting statistics limits the accuracy of this technique on Omega.

It is also possible to use the shape of the recoil or knock-on deuteron (KOD) spectrum following elastic (n, D) scattering in the fuel to infer the burn-averaged areal density.[26] These measurements are made along two lines of sight using charged-particle spectrometers (CPSs).[27] As shown by Frenje *et al.*,[26] the shape of the KOD spectrum evolves dramatically as the fuel areal density increases up to 180 $\mathrm{mg/cm^2}$. Above 180 $\mathrm{mg/cm^2}$, the shape of the spectrum no longer changes with increasing areal density, and the measurement is saturated, i.e., the $\langle \rho R \rangle_n$ is at least 180 $\mathrm{mg/cm^2}$.

A properly tuned version of the low-adiabat ($\alpha \sim 2$), triple-picket pulse shape shown in Fig. 3(a) has been used to drive cryogenic-DT implosions on Omega. The targets were energy scaled from the ignition design shown in Fig. 2(a). The Omega target was a nominally 860-μm-diameter, 10-μm thick CD shell filled with approximately 650 atm of DT (nominally 50:50) gas at standard temperature and pressure. When cooled to the triple point (approximately 18.7 K), the DT-ice layer inside the shell was about 65 μm thick. The targets were mounted on 17-μm-diameter SiC stalks. These stalk-mounted targets were more stable than earlier silk-mounted designs[8] during target alignment and the shot sequence. The higher-stiffness stalk provides considerably more damping of vibrations induced during target exposure. Subsequently, the stalk-mounted targets are, on average, much closer to target chamber center (TCC) at shot time than silk-mounted targets. Generally, target performance (yield, $\langle T_i \rangle_n$, and $\langle \rho R \rangle_n$) is impacted if the offset from TCC at shot time is larger than the hot-spot radius at peak compression.

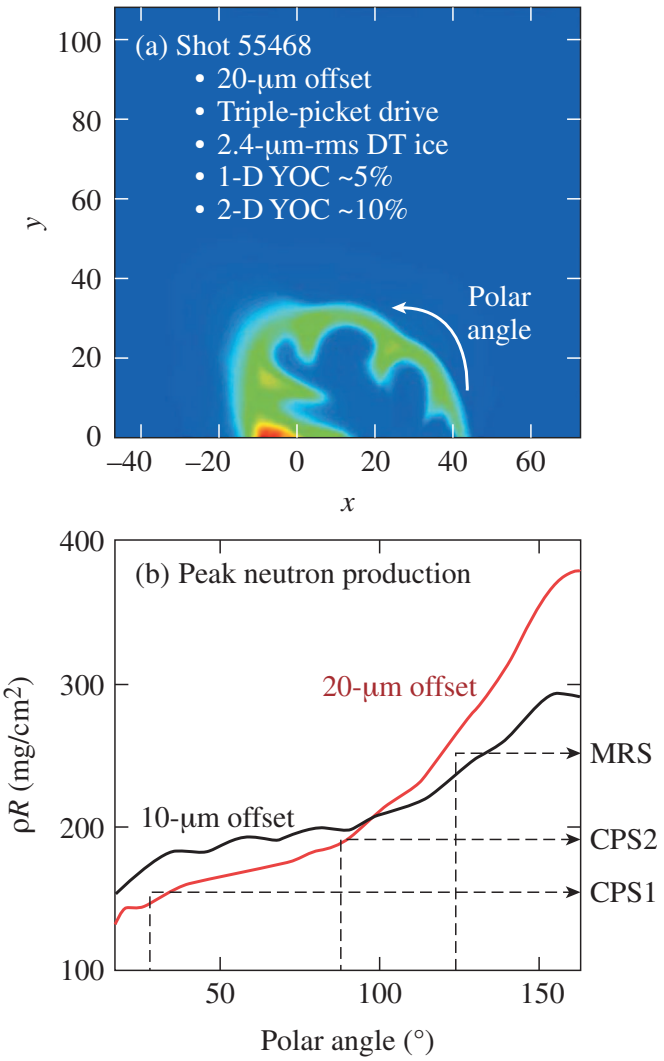

FIG. 4. (Color) (a) The DT-fuel-density distribution at peak burn for shot 55468 as predicted by the 2D radiation hydrocode DRACO using a measured offset of 20 μm. (b) $\langle \rho R \rangle_n$ along radial lines of sight from the center of the hot spot is plotted as a function of the angle measured from the $+x$ axis (red curve). The $\langle \rho R \rangle_n$ variation as a function of the polar angle is a factor of 3 and agrees well with the measured values listed in Table I. The black curve is an identical simulation for an offset of 10 μm and shows that a single line-of-sight measurement using the MRS would provide a reasonable estimate of the average $\langle \rho R \rangle_n$ for such an implosion.

The impact of the target offset relative to TCC at shot time is shown in Fig. 4 and Table I. Figure 4(a) shows a 2D radiation hydrodynamics code (DRACO) simulation of shot 55468 on Omega [the target was as described above; the pulse shape was a slightly higher adiabat version of the triple-picket pulse shown in Fig. 3(a)]. The target offset at shot time was measured to be approximately 20 μm using fixed time-integrated x-ray pinhole cameras.[28] The simulation incorporates the offset along the $+x$ axis, and the figure shows the fuel-density distribution at peak compression. The

TABLE I. The measured and predicted values for the $\langle \rho R \rangle_n$ on shot 55468.

Measurement	Experimental (mg/cm^2)	DRACO 2D (mg/cm^2)	Fraction of 2D ρR measured
MRS	~220	~250	~90%
CPS2	>180	~190	~100%
CPS1	~170	~160	~100%

hot-spot radius was comparable to the magnitude of the offset. Calculating the $\langle \rho R \rangle_n$ along lines of sight from the center of the hot spot through the dense shell for all "polar" angles (where 0° was measured from the $+x$ axis of the offset direction) resulted in the red curve in Fig. 4(b). The predicted $\langle \rho R \rangle_n$ in mg/cm^2 is plotted as a function of this polar angle and shows that even for a relatively small target offset (20 μm), the variation in the areal density can be as much as a factor of 3. Table I lists the experimentally inferred $\langle \rho R \rangle_n$ for CPS1, CPS2, and the MRS, the corresponding 2D-predicted $\langle \rho R \rangle_n$ along the lines of sight of the instruments, and the fraction of the predicted measured $\langle \rho R \rangle_n$. For this shot (and others as well) the measured areal-density variation was consistent with the 2D prediction (it should be noted that neither the CPS nor the MRS are line-of-sight measurements of the areal density; this comparison is possible because the areal-density variation across the effective solid angle of the measurement is relatively small). The black curve in Fig. 4(b) is the 2D simulation using a 10-μm offset. In this case, the variation with angle is fairly small and a single line-of-sight measurement with the MRS (for $\langle \rho R \rangle_n > 180$ mg/cm^2) would be representative of the average fuel $\langle \rho R \rangle_n$. The goal for target offsets on Omega experiments is 10 μm or less from TCC.

At present, stalk-mounted targets can be used only with DT fuel. The native β-layering process[8,29] is only marginally affected by the small thermal perturbation introduced by the stalk. The average layer quality of the stalk-mounted DT targets imploded to date is 1.9-μm rms in all modes with the dominant feature being a slight thickening of the ice above the stalk (the stalk tends to be slighter cooler than the target). Layer quality with stalk-mounted D_2 targets has not (so far) been adequate for target physics. D_2 fuel requires enhanced IR layering;[30] the lack of uniform IR illumination coupled with energy absorbed by the stalk (despite using IR transparent materials) has limited the best ice layers to a 4–5-μm rms range. Initial tests using IR illumination of a stalk-mounted DT target suggest, however, that the temperature of the stalk can be brought into equilibrium with the capsule (the IR wavelength is tuned to preferentially heat the stalk), resulting in sub-1-μm rms layer qualities. Modifications are underway to provide IR illumination for all future DT targets.

Figure 5 shows (a) the CPS1 KOD spectrum, (b) the CPS2 KOD spectrum, and (c) the MRS deuteron spectrum for a recent implosion using a properly tuned version of the pulse shape in Fig. 3(a) and the target described above. The KOD shapes are similar and, according to Ref. 26, fully saturated, indicating that the $\langle \rho R \rangle_n$ along these two (roughly orthogonal) lines of sight was at least 180 mg/cm^2. The MRS deuteron spectrum is best fit using a $\langle \rho R \rangle_n$ of approximately 290–300 mg/cm^2. The two points at 7 and 8 MeV are from neutrons scattered in the dense fuel; the broad peak centered at 11–12 MeV are from the primary neutrons. The width of the peak is dominated by the response of the MRS. A neutron spectrum consistent with a $\langle \rho R \rangle_n$ of 290–300 mg/cm^2 is convolved with the response function to give the fitted line. The relatively large error bar is dominated by the statistical

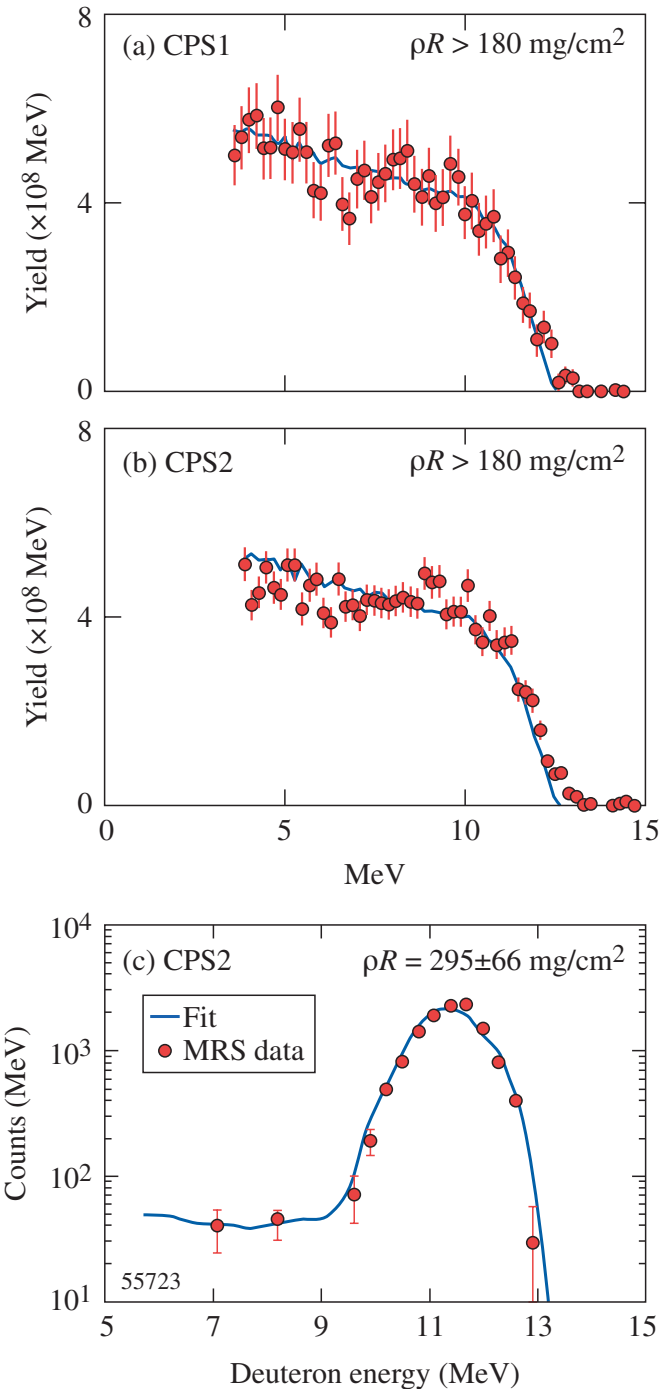

FIG. 5. (Color) (a) The CPS1 and (b) CPS2 spectra for shot 55723 are fully saturated, i.e., the shape of the spectra is independent of $\langle \rho R \rangle_n$. The MRS (c) deuteron spectrum shows the downscattered and primary yields leading to an inferred value of the $\langle \rho R \rangle_n$ of approximately 300 ± 60 mg/cm^2.

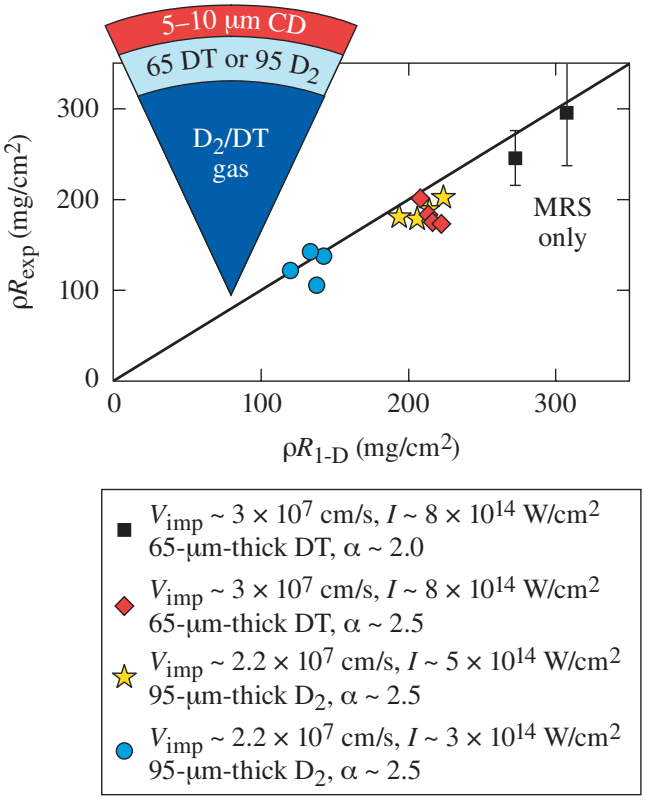

FIG. 6. (Color) The experimental $\langle \rho R \rangle_n$ is plotted as a function of the 1D-predicted $\langle \rho R \rangle_n$ for a variety of drive conditions and target designs.

error of the two points at 7 and 8 MeV. The target offset for this implosion was less than 10 μm.

Figure 6 shows a summary to date of the high-$\langle \rho R \rangle_n$ cryogenic-DT implosions on Omega. The experimentally inferred $\langle \rho R \rangle_n$ is plotted as a function of the burn-averaged prediction of LILAC [the one-dimensional (1D) radiation hydrodynamics code]. The blue circles and yellow stars are earlier data using continuous drive pulses and D_2 fuel;[7] as discussed in Sec. I, these designs do not scale to ignition. The data for the black square near 300 mg/cm^2 are shown in Fig. 4; the other point at approximately 240 mg/cm^2 was an identical implosion, except that the second picket energy was higher than requested, raising the adiabat and reducing the predicted and experimentally inferred areal density. The CPS KOD data for both implosions were saturated. The target offset for the 240-mg/cm^2 implosion was less than 20 μm. The red diamonds are four nearly identical implosions using a pulse shape without the small notch in the main drive. The design adiabat was approximately 2.5, and the 1D-predicted burn-averaged areal densities ranged from 210 to 220 mg/cm^2. For these points, the experimentally inferred $\langle \rho R \rangle_n$ was the average of the CPS KOD measurements (up to 180 mg/cm^2) and the corresponding MRS value. The TCC offsets for these points were less than 20 μm. The experimentally inferred $\langle \rho R \rangle_n$ for all of the DT implosions was approximately 90% of the 1D prediction, indicating that the fuel assembly proceeded according to the simulation up to the point of burn truncation[6] (the yields of these implosions were 3%–6% of the 1D prediction); as the yield began to quench due to cold fuel mixing into the hot spot, the peak densities were not fully sampled by the emitted neutrons.

The $\langle T_i \rangle_n$ for the implosions shown in Fig. 6 was inferred using neutron time-of-flight spectroscopy.[31] The relative accuracy of these measurements shot-to-shot is approximately 0.1–0.2 keV depending on the measurement configuration and the neutron-hit statistics in the various detectors. The $\langle T_i \rangle_n$ for the 240- and 300-mg/cm^2 points in Fig. 6 was 1.8 keV; for the cluster of points around 200 mg/cm^2, the $\langle T_i \rangle_n$ ranged from 2.0 to 2.2 keV, independent of the fuel type. It appears that the $\langle T_i \rangle_n$ was lower for the lower-adiabat, higher-compression implosions. This is consistent with the smaller predicted hot spot and greater cold-fuel mixing in the hot spot expected for the higher-compression implosions. The mixing was the result of laser and target perturbations, including ice roughness, laser-drive nonuniformity (primarily pointing- and single-beam nonuniformity), capsule-surface imperfections associated with the stalk mount, and target offsets comparable to the hot-spot radius. While work continues to improve on these intrinsic nonuniformities (e.g., IR heating has been shown to improve the ice-layer smoothness by 2×), it may not be possible to achieve a $\langle T_i \rangle_n$ of ~3.4 keV on Omega. Further work will be performed to quantify these effects on the ignition hydroequivalence requirements for Omega implosions.

IV. SUMMARY

A new multiple-picket, multiple-shock drive pulse has been used to implode cryogenic-DT targets at implosion velocities that scale to ignition on the NIF. The $\langle \rho R \rangle_n$ reported here are very close to the predictions of the 1D hydrocode LILAC, suggesting that accurate control over the adiabat can be maintained by careful tuning of the shock velocities and coalescence times in the fuel. The best of the $\alpha \sim 2$ implosions led to a measured $\langle \rho R \rangle_n$ of 300 ± 60 mg/cm^2, the minimum areal density required to generate a thermonuclear burn wave. The predicted (LILAC) peak density for this implosion is 250 g/cm^3, corresponding to 1000× liquid density. This is the highest ICF fuel density achieved in laboratory-based experiments.

A $\langle \rho R \rangle_n$ of 300 mg/cm^2 is also one of the two primary requirements for demonstrating ignition hydrodynamic equivalence on the NIF. For $\alpha \sim 2$ implosions, an $\langle T_i \rangle_n$ of 3.4 keV and a $\langle \rho R \rangle_n$ of 300 mg/cm^2 would scale to ignition with a laser energy of 500 kJ (well within the capabilities of the NIF). An implosion velocity of approximately 3.5×10^7 cm/s will be needed to achieve this ion temperature. Intrinsic target and laser nonuniformities on Omega may ultimately limit the maximum achievable $\langle T_i \rangle_n$. Further work on the ICF "Betti ignition criteria"[15] may lead to a relaxed requirement on $\langle T_i \rangle_n$ (due to multidimensional effects) for the demonstration of ignition hydrodynamic equivalence with DT cryogenic implosions on Omega.

ACKNOWLEDGMENTS

This work was supported by the U.S. Department of Energy Office of Inertial Confinement Fusion under Cooperative Agreement No. DE-FC52-08NA28302, the University of Rochester, and the New York State Energy Research and Development Authority.

[1] W. J. Hogan, E. I. Moses, B. E. Warner, M. S. Sorem, and J. M. Soures, Nucl. Fusion **41**, 567 (2001).
[2] S. W. Haan, D. A. Callahan, M. J. Edwards, B. A. Hammel, D. D. Ho, O. S. Jones, J. D. Lindl, B. J. MacGowan, M. M. Marinak, D. H. Munro, S. M. Pollaine, J. D. Salmonson, B. K. Spears, and L. J. Suter, Fusion Sci. Technol. **55**, 227 (2009).
[3] T. R. Boehly, D. L. Brown, R. S. Craxton, R. L. Keck, J. P. Knauer, J. H. Kelly, T. J. Kessler, S. A. Kumpan, S. J. Loucks, S. A. Letzring, F. J. Marshall, R. L. McCrory, S. F. B. Morse, W. Seka, J. M. Soures, and C. P. Verdon, Opt. Commun. **133**, 495 (1997).
[4] V. A. Smalyuk, R. Betti, T. R. Boehly, R. S. Craxton, J. A. Delettrez, D. H. Edgell, V. Yu. Glebov, V. N. Goncharov, D. R. Harding, S. X. Hu, J. P. Knauer, F. J. Marshall, R. L. McCrory, P. W. McKenty, D. D. Meyerhofer, P. B. Radha, S. P. Regan, T. C. Sangster, W. Seka, R. W. Short, D. Shvarts, S. Skupsky, J. M. Soures, C. Stoeckl, B. Yaakobi, J. A. Frenje, C. K. Li, R. D. Petrasso, and F. H. Séguin, Phys. Plasmas **16**, 056301 (2009).
[5] R. L. McCrory, D. D. Meyerhofer, R. Betti, R. S. Craxton, J. A. Delettrez, D. H. Edgell, V. Yu Glebov, V. N. Goncharov, D. R. Harding, D. W. Jacobs-Perkins, J. P. Knauer, F. J. Marshall, P. W. McKenty, P. B. Radha, S. P. Regan, T. C. Sangster, W. Seka, R. W. Short, S. Skupsky, V. A. Smalyuk, J. M. Soures, C. Stoeckl, B. Yaakobi, D. Shvarts, J. A. Frenje, C. K. Li, R. D. Petrasso, and F. H. Séguin, Phys. Plasmas **15**, 055503 (2008).
[6] V. N. Goncharov, T. C. Sangster, P. B. Radha, R. Betti, T. R. Boehly, T. J. B. Collins, R. S. Craxton, J. A. Delettrez, R. Epstein, V. Yu. Glebov, S. X. Hu, I. V. Igumenshchev, J. P. Knauer, S. J. Loucks, J. A. Marozas, F. J. Marshall, R. L. McCrory, P. W. McKenty, D. D. Meyerhofer, S. P. Regan, W. Seka, S. Skupsky, V. A. Smalyuk, J. M. Soures, C. Stoeckl, D. Shvarts, J. A. Frenje, R. D. Petrasso, C. K. Li, F. Séguin, W. Manheimer, and D. G. Colombant, Phys. Plasmas **15**, 056310 (2008).
[7] T. C. Sangster, V. N. Goncharov, P. B. Radha, V. A. Smalyuk, R. Betti, R. S. Craxton, J. A. Delettrez, D. H. Edgell, V. Yu. Glebov, D. R. Harding, D. Jacobs-Perkins, J. P. Knauer, F. J. Marshall, R. L. McCrory, P. W. McKenty, D. D. Meyerhofer, S. P. Regan, W. Seka, R. W. Short, S. Skupsky, J. M. Soures, C. Stoeckl, B. Yaakobi, D. Shvarts, J. A. Frenje, C. K. Li, R. D. Petrasso, and F. H. Séguin, Phys. Rev. Lett. **100**, 185006 (2008).
[8] T. C. Sangster, R. Betti, R. S. Craxton, J. A. Delettrez, D. H. Edgell, L. M. Elasky, V. Yu. Glebov, V. N. Goncharov, D. R. Harding, D. Jacobs-Perkins, R. Janezic, R. L. Keck, J. P. Knauer, S. J. Loucks, L. D. Lund, F. J. Marshall, R. L. McCrory, P. W. McKenty, D. D. Meyerhofer, P. B. Radha, S. P. Regan, W. Seka, W. T. Shmayda, S. Skupsky, V. A. Smalyuk, J. M. Soures, C. Stoeckl, B. Yaakobi, J. A. Frenje, C. K. Li, R. D. Petrasso, F. H. Séguin, J. D. Moody, J. A. Atherton, B. D. MacGowan, J. D. Kilkenny, T. P. Bernat, and D. S. Montgomery, Phys. Plasmas **14**, 058101 (2007).
[9] V. A. Smalyuk, S. B. Dumanis, J. A. Delettrez, V. Yu. Glebov, D. D. Meyerhofer, S. P. Regan, T. C. Sangster, and C. Stoeckl, Phys. Plasmas **13**, 104502 (2006).
[10] F. J. Marshall, R. S. Craxton, J. A. Delettrez, D. H. Edgell, L. M. Elasky, R. Epstein, V. Yu. Glebov, V. N. Goncharov, D. R. Harding, R. Janezic, R. L. Keck, J. D. Kilkenny, J. P. Knauer, S. J. Loucks, L. D. Lund, R. L. McCrory, P. W. McKenty, D. D. Meyerhofer, P. B. Radha, S. P. Regan, T. C. Sangster, W. Seka, V. A. Smalyuk, J. M. Soures, C. Stoeckl, S. Skupsky, J. A. Frenje, C. K. Li, R. D. Petrasso, and F. H. Séguin, Phys. Plasmas **12**, 056302 (2005).
[11] V. A. Smalyuk, J. A. Delettrez, S. B. Dumanis, R. Epstein, V. Yu. Glebov, D. D. Meyerhofer, P. B. Radha, T. C. Sangster, C. Stoeckl, N. C. Toscano, J. A. Frenje, C. K. Li, R. D. Petrasso, F. H. Séguin, and J. A. Koch, Phys. Plasmas **12**, 052706 (2005).
[12] P. W. McKenty, T. C. Sangster, M. Alexander, R. Betti, R. S. Craxton, J. A. Delettrez, L. Elasky, R. Epstein, A. Frank, V. Yu. Glebov, V. N. Goncharov, D. R. Harding, S. Jin, J. P. Knauer, R. L. Keck, S. J. Loucks, L. D. Lund, R. L. McCrory, F. J. Marshall, D. D. Meyerhofer, S. P. Regan, P. B. Radha, S. Roberts, W. Seka, S. Skupsky, V. A. Smalyuk, J. M. Soures, K. A. Thorp, M. Wozniak, J. A. Frenje, C. K. Li, R. D. Petrasso, F. H. Séguin, K. A. Fletcher, S. Padalino, C. Freeman, N. Izumi, J. A. Koch, R. A. Lerche, M. J. Moran, T. W. Phillips, G. J. Schmid, and C. Sorce, Phys. Plasmas **11**, 2790 (2004).
[13] T. C. Sangster, J. A. Delettrez, R. Epstein, V. Yu. Glebov, V. N. Goncharov, D. R. Harding, J. P. Knauer, R. L. Keck, J. D. Kilkenny, S. J. Loucks, L. D. Lund, R. L. McCrory, P. W. McKenty, F. J. Marshall, D. D. Meyerhofer, S. F. B. Morse, S. P. Regan, P. B. Radha, S. Roberts, W. Seka, S. Skupsky, V. A. Smalyuk, C. Sorce, J. M. Soures, C. Stoeckl, K. Thorp, J. A. Frenje, C. K. Li, R. D. Petrasso, F. H. Séguin, K. A. Fletcher, S. Padalino, C. Freeman, N. Izumi, J. A. Koch, R. A. Lerche, M. J. Moran, T. W. Phillips, and G. J. Schmid, Phys. Plasmas **10**, 1937 (2003).
[14] C. Stoeckl, C. Chiritescu, J. A. Delettrez, R. Epstein, V. Yu. Glebov, D. R. Harding, R. L. Keck, S. J. Loucks, L. D. Lund, R. L. McCrory, P. W. McKenty, F. J. Marshall, D. D. Meyerhofer, S. F. B. Morse, S. P. Regan, P. B. Radha, S. Roberts, T. C. Sangster, W. Seka, S. Skupsky, V. A. Smalyuk, C. Sorce, J. M. Soures, R. P. J. Town, J. A. Frenje, C. K. Li, R. D. Petrasso, F. H. Séguin, K. Fletcher, S. Padalino, C. Freeman, N. Izumi, R. Lerche, and T. W. Phillips, Phys. Plasmas **9**, 2195 (2002).
[15] R. Betti, K. S. Anderson, P. Y. Chang, R. Nora, C. D. Zhou, B. Spears, J. Edwards, S. W. Haan, and J. Lindl, Phys. Plasmas **17**, 058102 (2010).
[16] C. D. Zhou and R. Betti, Phys. Plasmas **15**, 102707 (2008).
[17] J. D. Lawson, Proc. Phys. Soc. London **B70**, 6 (1957).
[18] J. D. Lindl, *Inertial Confinement Fusion: The Quest for Ignition and Energy Gain Using Indirect Drive* (Springer-Verlag, New York, 1998).
[19] C. D. Zhou and R. Betti, Phys. Plasmas **14**, 072703 (2007).
[20] M. C. Herrmann, M. Tabak, and J. D. Lindl, Nucl. Fusion **41**, 99 (2001).
[21] V. N. Goncharov, T. C. Sangster, T. R. Boehly, S. X. Hu, I. V. Igumenshchev, F. J. Marshall, R. L. McCrory, D. D. Meyerhofer, P. B. Radha, W. Seka, S. Skupsky, C. Stoeckl, D. T. Casey, J. A. Frenje, and R. D. Petrasso, Phys. Rev. Lett. **104**, 165001 (2010).
[22] T. R. Boehly, D. H. Munro, P. M. Celliers, R. E. Olson, D. G. Hicks, V. N. Goncharov, G. W. Collins, H. F. Robey, S. X. Hu, J. A. Marozas, T. C. Sangster, O. L. Landen, and D. D. Meyerhofer, Phys. Plasmas **16**, 056302 (2009).
[23] R. Tommasini, A. MacPhee, D. Hey, T. Ma, C. Chen, N. Izumi, W. Unites, A. MacKinnon, S. P. Hatchett, B. A. Remington, H. S. Park, P. Springer, J. A. Koch, O. L. Landen, J. Seely, G. Holland, and L. Hudson, Rev. Sci. Instrum. **79**, 10E901 (2008).
[24] J. A. Frenje, D. T. Casey, C. K. Li, J. R. Rygg, F. H. Séguin, R. D. Petrasso, V. Yu. Glebov, D. D. Meyerhofer, T. C. Sangster, S. Hatchett, S. Haan, C. Cerjan, O. Landen, M. Moran, P. Song, D. C. Wilson, and R. J. Leeper, Rev. Sci. Instrum. **79**, 10E502 (2008).
[25] J. A. Frenje, K. M. Green, D. G. Hicks, C. K. Li, F. H. Séguin, R. D. Petrasso, T. C. Sangster, T. W. Phillips, V. Yu. Glebov, D. D. Meyerhofer, S. Roberts, J. M. Soures, C. Stoeckl, K. Fletcher, S. Padalino, and R. J. Leeper, Rev. Sci. Instrum. **72**, 854 (2001).
[26] J. A. Frenje, C. K. Li, F. H. Séguin, D. T. Casey, R. D. Petrasso, T. C. Sangster, R. Betti, V. Yu. Glebov, and D. D. Meyerhofer, Phys. Plasmas **16**, 042704 (2009).
[27] F. H. Séguin, J. A. Frenje, C. K. Li, D. G. Hicks, S. Kurebayashi, J. R. Rygg, B.-E. Schwartz, R. D. Petrasso, S. Roberts, J. M. Soures, D. D. Meyerhofer, T. C. Sangster, J. P. Knauer, C. Sorce, V. Yu. Glebov, C. Stoeckl, T. W. Phillips, R. J. Leeper, K. Fletcher, and S. Padalino, Rev. Sci. Instrum. **74**, 975 (2003).
[28] F. J. Marshall, T. Ohki, D. McInnis, Z. Ninkov, and J. Carbone, Rev. Sci. Instrum. **72**, 713 (2001).
[29] J. K. Hoffer and L. R. Foreman, Phys. Rev. Lett. **60**, 1310 (1988).
[30] G. W. Collins, D. N. Bittner, E. Monsler, S. Letts, E. R. Mapoles, and T. P. Bernat, J. Vac. Sci. Technol. A **14**, 2897 (1996).
[31] T. J. Murphy, R. E. Chrien, and K. A. Klare, Rev. Sci. Instrum. **68**, 610 (1997).